

Correlation between tensile and bending behavior of FRC composites with scale effect

D.J. Kim

Sejong University, Seoul, South Korea

A.E. Naaman & S. El-Tawil

University of Michigan, Ann Arbor, MI, USA

ABSTRACT: This paper describes the results of an experimental test program designed to correlate the tensile and bending response of fiber reinforced cement composites tested under the same conditions. Several objectives were sought: 1) to correlate tensile and bending behavior of specimens having about the same cross section; 2) to ascertain that a strain hardening composite in tension leads surely to a deflection hardening composite in bending; 3) to observe scale effects on bending behavior; and 4) to verify if some theoretical correlation between post-cracking tensile strength and bending resistance (modulus of rupture) are validated by experiments. The final objective of this study is to provide hard data needed to determine if the tensile stress-strain response of fiber reinforced cement composites can be predicted from their load-deflection response, as currently surmised in some test standards and in some finite element studies claiming that tensile response can be uniquely back-calculated from bending behavior. The test program included several parameters, among which 2 types of high strength steel fibers (hooked and twisted) with identical volume fractions of fibers (1%), and three different sizes of cross section for the beams, namely, 50×25 mm, 100×100 mm, and 150×150 mm. Key observations are described and conclusions drawn.

1 INSTRUCTIONS

Much research has been conducted to increase the ductility of cement based composites by adding short fibers, because cement based matrices have innate weakness in terms of brittle failure under tensile and flexural loading. To remedy such weakness, Fiber Reinforced Concrete (FRC) and High Performance Fiber Reinforced Cementitious Composites (HPFRCC) have been developed. FRC and HPFRCC are usually first differentiated by their uniaxial tensile response. FRC shows strain softening behavior under uniaxial tensile load while HPFRCC shows strain hardening behavior. (Naaman & Reinhardt 1996) Although all fiber reinforced cement composites can be simply characterized according to their tensile response, so far there is no standard tensile test method for fiber reinforced cement composites. Many researchers are still using different tensile test set-ups e.g., different boundary conditions, sizes and geometries of specimens, gage length, and measurement techniques. For example, some researchers have been using bell shaped tensile specimens with hinge to hinge boundary conditions while others have been using coupon type specimens with fixed boundary conditions. Since there is no standard tensile test method for FRC and HPFRCC, and since such test-

ing is more difficult to carry out, many researchers have investigated whether the third point flexural test can be used, as an alternative test method, to obtain the tensile response of the composite. Note that the flexural response can be predicted analytically from the tensile and compressive behavior of the material. (Naaman (2003), Soranakom (2007) & Mobasher, 2008)) However, it is questioned whether the tensile response of the composite can be uniquely back-calculated from its flexural response. An experimental test program was designed and carried out in order to: 1) correlate the tensile and bending behavior of FRC specimens with same cross section and to provide some data to the above question, and 2) to investigate the scale effect on bending behavior, and 3) to provide data for use by researchers attempting to predict tensile response from bending response.

2 DEFLECTION HARDENING AND STRAIN HARDENING

The response of a beam specimen under flexural loading contains structural effects due to the specimen geometry and loading conditions. For instance, although the tensile behavior of an FRC specimen may generate a strain softening response, it may also

generate either a deflection-softening or a deflection-hardening response due to the structural effect under flexural load. Naaman (2003) suggested a practical condition for deflection hardening response, when the post cracking strength (σ_{pc}) in tension is higher than the first cracking strength (σ_{cc}) multiplied with a factor, k , smaller than 1, i.e., $\sigma_{pc} \geq k\sigma_{cc}$. The factor k ranges between 1/3 and 1, with 0.4 being a recommended first approximation. Soranakom & Mobasher (2007) proposed a closed form solution for the moment-curvature response of FRC, and the simulation results, using their model, indicated that the direct use of uniaxial tensile stress – strain response under-predicts the flexural response. They explained this discrepancy by the difference in the strain gradient profile and the volume of the stressed region between the tensile and flexural tests. Soranakom & Mobasher (2008) also mentioned that the brittleness and size effect are more pronounced in the flexural response of brittle materials, while more accurate predictions are obtained with ductile materials. Therefore, in inverse estimating FRC tensile response from their flexural response, the size of flexural specimens should be carefully selected. It is well known that there is a strong size effect in the behavior of cementitious composites due to their brittle behavior (Bazant & Planas (1998), Bazant et al. (1994)). Ward & Li (1990) investigated the flexural behavior of fiber reinforced mortar beams of different sizes and proposed the ratio between flexural strength and tensile strength as a parameter to describe the brittleness of material. The ratio decreases as the brittleness of the material increases. Bazant et al. (1994), using extensive laboratory results, also concluded that all types of brittle failures of concrete structures exhibit a strong size effect. Lepech & Li (2004) investigated size effect in ECC structural (plain and reinforced with steel bars) beams and reported that there is negligible size effect in ECC compared to brittle concrete. However, the results were based only on comparing the equivalent elastic bending strength but did not consider the deflection capacity.

In evaluating the tensile behavior of ductile fiber reinforced cement composites, the strain capacity is a paramount parameter. Therefore, in this experimental program, the size effect in flexural members is investigated not only with respect to bending resistance but also to deflection capacity at peak stress.

3 EXPERIMENTAL PROGRAM

Two types of high strength steel fibers (Hooked and Twisted), showing slip hardening response under single fiber pull-out testing, were used in a high strength cementitious matrix (84MPa) with 1% fiber by volume. Tensile and bending specimens were

prepared. Direct tensile tests and flexural tests were carried out using a servo-controlled hydraulic testing machine (MTS810). All the tensile test series led to a strain-hardening behavior. For the flexural tests, three different geometries of specimens, S (small), M (medium), and L (large) were prepared to investigate the size effect on the flexural behavior of HPFRCC.

3.1 Materials and specimen preparation

The matrix mix composition and proportions are shown in Table 1, and the properties of fibers are shown in Table 2. A VMA (Viscosity Modifying Agent) was added to the matrix to increase viscosity and ensure uniform fiber distribution in the matrix. The compressive strength of the matrix was measured from 100x200 mm cylinders and this matrix was a self-consolidating mixture developed earlier.

Table 1. Matrix composition by weight ratio and compressive strength.

Cement (Type III)	0.80
Fly ash	0.20
Sand (Flint)	1.00
Silica fume	0.07
Super-Plasticizer	0.04
VMA	0.012
Water	0.26
f'_c (MPa)	84

Table 2. Properties of fibers used in this study.

Fiber type	Hooked	Twisted
Diameter (mm)	0.38	0.30*
Length (mm)	30	30
Density (g/cc)	7.9	7.9
Tensile strength (MPa)	2300	2760**
Elastic modulus (GPa)	200	200

* Equivalent diameter

** Tensile strength of the fiber after twisting

The geometry of the tensile test specimens and the test set-up are shown in Figure 1. Two layers of steel wire mesh were used to reinforce the bell shaped ends of the tensile specimens to minimize failure at the grips and out of the gage length. The gage length was selected to be 175mm (=7 inch), between two infrared markers; displacement between the markers was measured using a non-contacting motion measuring instrument (OPTOTRAK System) placed at about one meter from the specimen; the measurement accuracy was 0.001 mm. Beams of three different

geometries were prepared for the flexural tests (Fig. 2): S ($50\text{mm}\times 25\text{mm}\times 300\text{mm}$); M ($100\text{mm}\times 100\text{mm}\times 300\text{mm}$); & L ($150\text{mm}\times 150\text{mm}\times 450\text{mm}$). In addition to M and L type specimens, which are recommended in ASTM C1609, the S type beam specimens were intentionally added in this experimental program in order to have same cross sectional area as the tensile specimens.

3.2 Test setups and procedure

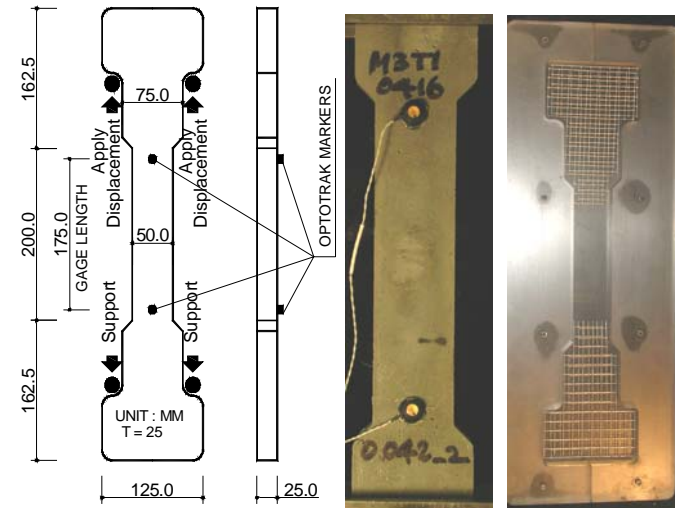


Figure 1. Tensile test specimen and setup.

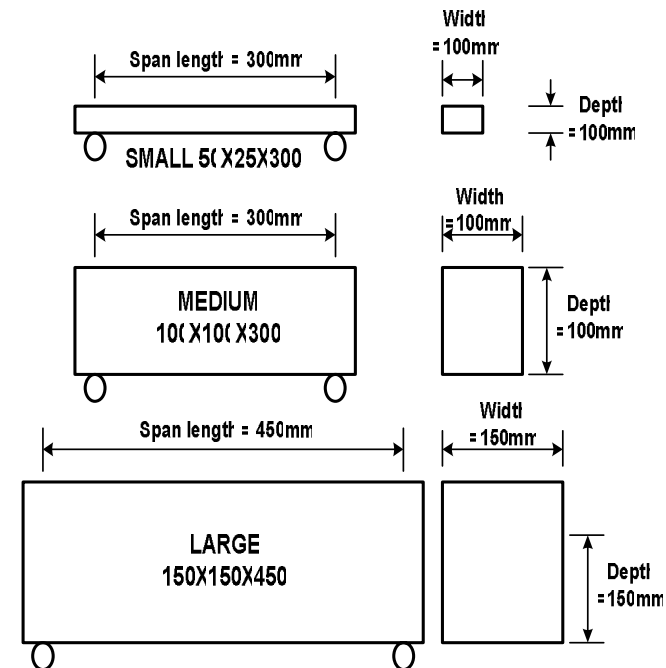
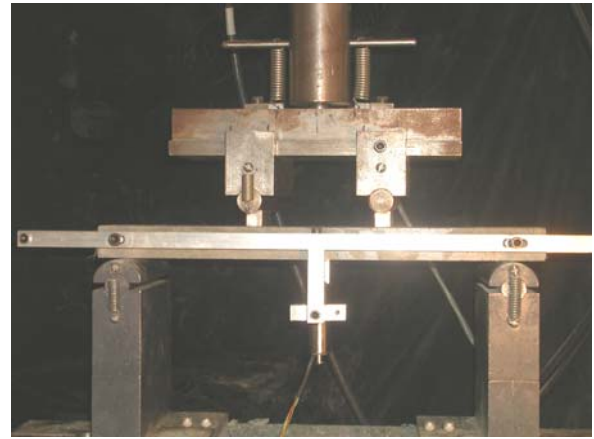
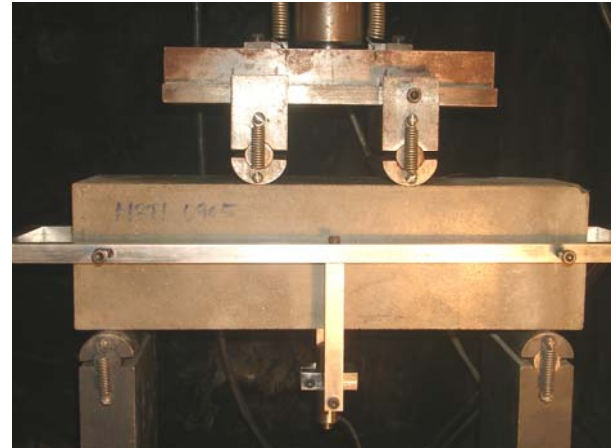


Figure 2. Three types of flexural test specimens.

Photos illustrating test set-ups for the flexural specimens are shown in Figure 3. Detailed information about the flexural test set-up can be found in Kim et al. (2008). The loading speed for both tensile and flexural tests, i.e. 1.06 mm/min , was originally determined from the tensile test by assuming that the static strain rate is $0.0001/\text{sec}$ which is actually ten times faster than the flexural loading speed recommended in ASTM C1609. The intention of applying same loading speed for both tensile and flexural tests was to minimize its effect on the observed results.



(a) S type ($50\text{mm}\times 25\text{mm}\times 300\text{mm}$)



(b) M Type ($100\text{mm}\times 100\text{mm}\times 300\text{mm}$)



(c) L type ($150\text{mm}\times 150\text{mm}\times 450\text{mm}$)

Figure 3. Test set-ups for flexural tests with different specimen sizes.

Photos illustrating test set-ups for the flexural specimens are shown in Figure 3. Detailed information about the flexural test set-up can be found in Kim et al. (2008). The loading speed for both tensile and flexural tests, i.e. 1.06 mm/min , was originally determined from the tensile test by assuming that the static strain rate is $0.0001/\text{sec}$ which is actually ten times faster than the flexural loading speed recommended in ASTM C1609. The intention of applying same loading speed for both tensile and flexural tests was to minimize its effect on the observed results.

3.3 Test results

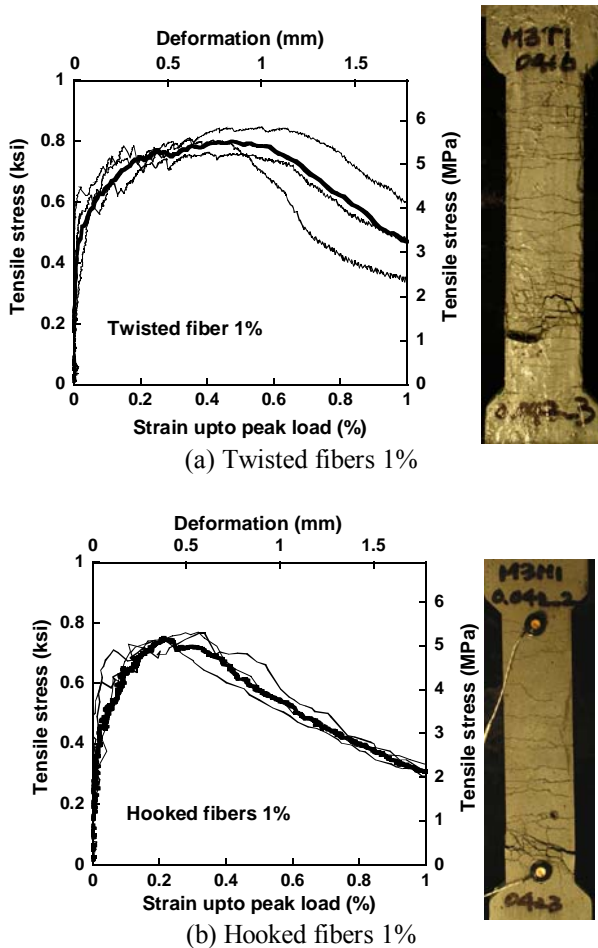


Figure 4. Tensile behavior of both Twisted and Hooked fibers reinforced specimen (Kim et al. 2008).

Table 3. Average experimental results obtained from the tensile tests (Kim et al. 2008).

Fiber type & volume content	Hooked 1%	Twisted 1%
First cracking strength (MPa)	4.299	4.264
Post cracking strength (MPa)	5.207	5.499
Strain capacity (%)	0.301	0.616
Number of cracks (EA)	15	23
Crack spacing (mm)	11.85	7.74
Average crack width (μm)	37	49

Tensile stress-strain curves (strain is valid up to peak stress only) of the test series with Twisted and Hooked fiber are shown in Figs. 4a and 4b, respectively. The average values of tensile parameters are estimated from at least three specimens and summarized in Table 3. These parameters include first cracking strength, post cracking strength, strain capacity at post-cracking strength, number of cracks within the gauge length, and average crack width. Crack spacing and average crack width were estimated from the total crack length within the gage length [Kim et al. 2008]. Since the modulus of rupture (MOR) under bending is highly correlated with

the post cracking tensile strength of FRC, post cracking strength values for both Twisted and Hooked fibers should be noted, i.e., the post cracking strength with Twisted fibers is about 5.5MPa while that with Hooked was about 5.2MPa.

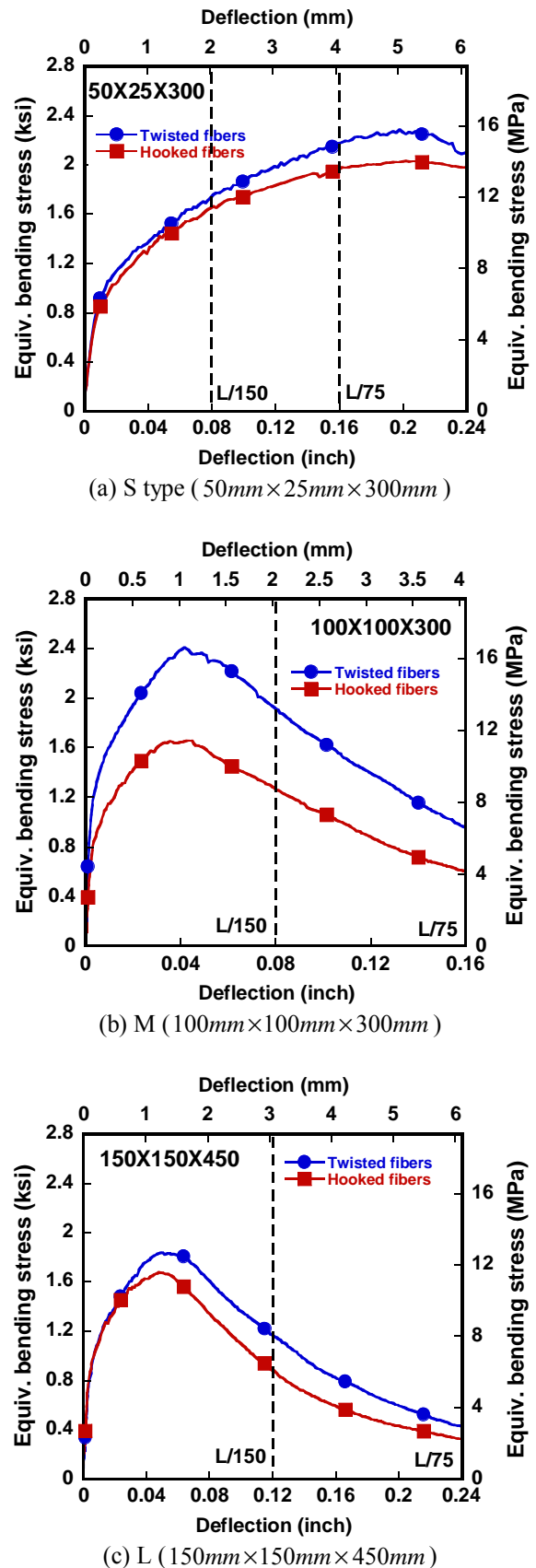


Figure 5. Flexural responses of Twisted and Hooked fiber reinforced specimens.

The flexural responses of test series with Twisted and Hooked fibers are shown in Figures 5a, 5b, and 5c according to the size of specimens, respectively. All of the results shown in Figure 5 are averages from three to six specimens.

Equivalent elastic bending strength is calculated from the following equation suggested in ASTM C1609.

$$f = \frac{PL}{bh^2} \quad (1)$$

where, f is equivalent bending stress; P is the applied load; b is the width of the specimen; and h is the depth of the specimen.

In referring to Figure 5, it is first observed that all specimens generated deflection hardening behavior accompanied by multiple cracks which appeared on the bottom and side surfaces of the specimens. The deflection hardening behavior was anticipated since the tensile behavior of these composites using Twisted and Hooked fibers produced strain hardening response under uniaxial tensile load (Fig. 4). Generally, the specimens reinforced with Twisted fibers produced higher equivalent bending strength than the specimens reinforced with Hooked fibers, as expected from their tensile response (Fig. 4). Equivalent bending strengths of specimens reinforced with Twisted fibers are 15.79MPa for S, 16.63MPa for M, and 12.70MPa for L series, while those with of Hooked fibers are 14.02MPa for S, 11.45MPa for M, and 11.56MPa for L series, respectively.

4 EVALUATION OF THE EXPERIMENTAL RESULTS

Although the flexural response of all test series shows deflection hardening behavior regardless of their different geometry, noticeable difference is observed in maximum equivalent bending strength, deflection capacity, and energy absorption capacity according to the different geometry.

Deflection capacity is defined as the deflection value at maximum equivalent bending stress and has a strong influence on the energy absorption capacity in flexure. Since the span length of each series of specimens is different according to their geometry (S, M, or L), the deflection values are normalized by the length of span for comparison as shown in Figure 6.

In addition, the equivalent bending strength is normalized by the post cracking tensile strength since there is difference in tensile strength between the test series with Twisted or Hooked fibers.

Normalized equivalent bending strength versus normalized deflection curves are graphically shown in

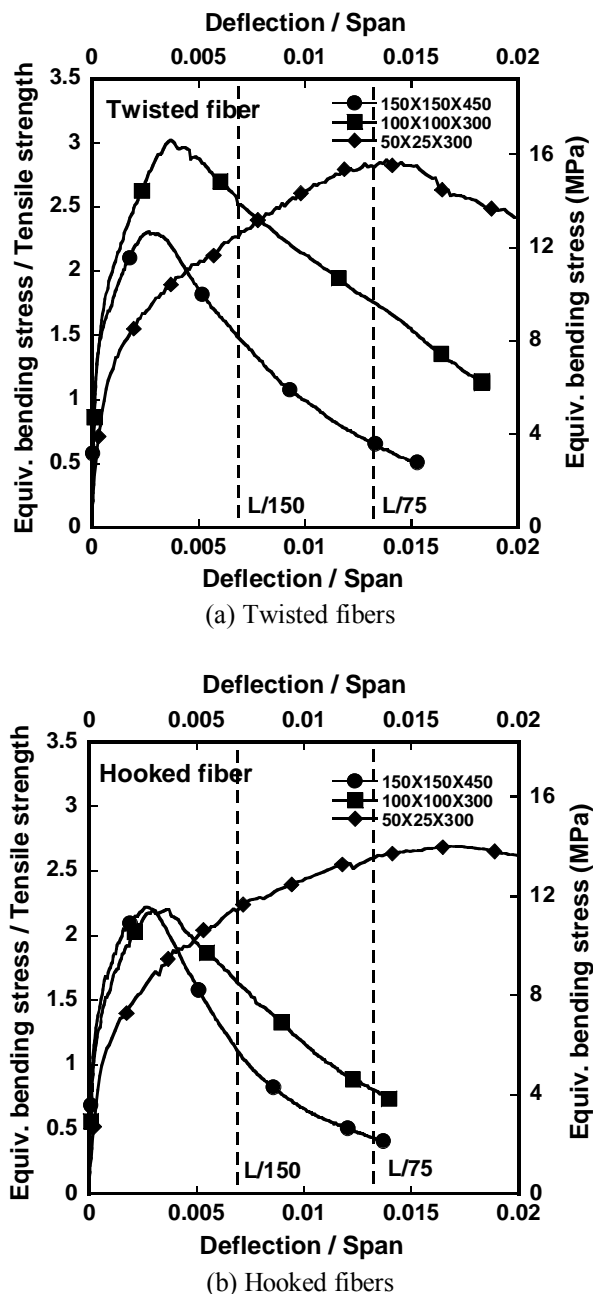


Figure 6. Equivalent bending stress versus normalized deflection curves.

Figure 6 and the cracking behavior of typical specimens is illustrated in Figure 7.

It can be observed from Figure 6 that both equivalent bending strength and deflection capacity decrease as the size of specimen increases. The deflection capacity of S type specimens is higher than L/75, while the deflection capacity of M and L type specimens is lower than L/150. Moreover, the deflection capacity of M type specimens is generally higher than that of L type specimens although the difference is small. The maximum equivalent bending strength also shows strong size dependency. Normalized equivalent bending strength of Twisted fibers reinforced specimens are 2.87 for S, 3.02 for M, and 2.31 for L sizes, while that of Hooked fibers reinforced specimens are 2.69 for S, 2.20 for M, and 2.22 for L sizes, respectively. The range of normalized equivalent bending strength is 2.20 to 3.02, and

this range is reasonable according to theoretical predictions (Naaman, 2003)

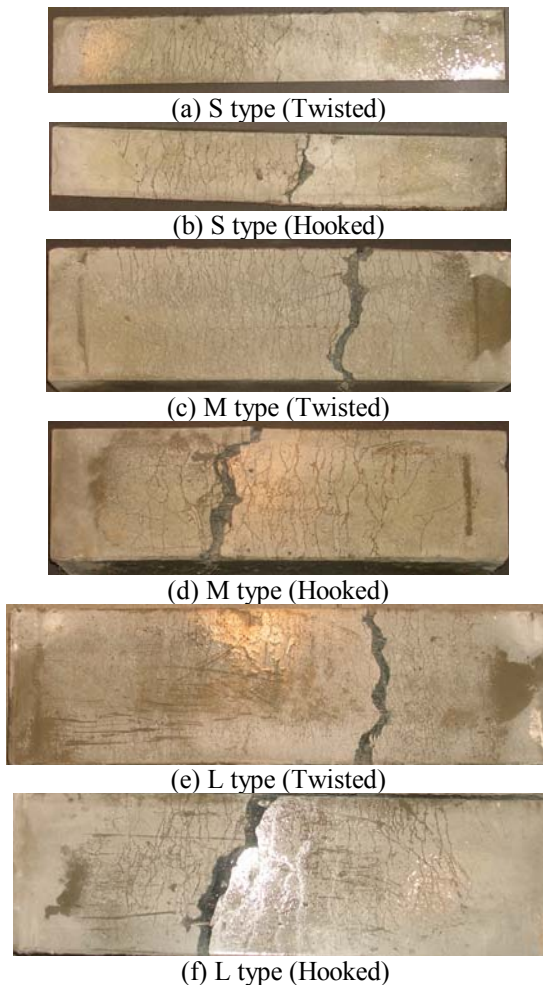


Figure 7. Cracking behavior of flexural specimens.

Given the above results, it is not clear that the flexural response can be used in order to predict the tensile behavior of material, uniquely. This is because the bending tests produced a strong size dependency not only for their bending strength but also their deflection capacity and their span length or span to depth ratio.

5 CONCLUSIONS

This study investigated the correlation between tensile and bending behavior of FRC Composites with scale effect by using three different geometries.

- Although test series with both Hooked and Twisted (Torex) fibers show deflection hardening behavior under flexural load, Twisted (Torex) fiber led generally to higher equivalent bending strength and deflection capacity.
- Maximum equivalent bending strength of S type specimen, which has same cross-sectional area as the tensile specimen, was almost three times higher than the post-cracking tensile strength obtained

from direct tensile tests. This is very close to analytically predicted best case conditions (Naaman, 2003).

- As the size of specimen decreases, both the equivalent bending strength and the deflection capacity increase.
- The ratio of equivalent bending strength to direct tensile strength for all test series ranged from about 2.2 to 3, which is well within the range predicted analytically (Naaman, 2003)
- This limited investigation suggests that tensile response cannot be uniquely predicted from bending response without consideration to size effect and span length or span to depth ratio.

It is hoped that additional studies will be carried out in the future to provide additional data to further resolve whether the tensile response can be uniquely predicted from the bending response, and if so, which parameters are needed.

6 ACKNOWLEDGEMENTS

The research described herein was sponsored by the US National Science Foundation under Grant No. CMS 0754505 to the University of Michigan. The opinions expressed in this paper are those of the authors and do not necessarily reflect the views of the sponsor.

REFERENCES

- ASTM C 1609/C 1690M-05, 2006, Standard test method for flexural performance of fiber reinforced concrete (using beam with third-point loading). American Society of Testing and Materials, pp. 1-8.
- Bazant, Z. P., Ozbolt, J. & Eligehausen, R., 1994, Fracture size effect: Review of evidence for concrete structures, *ASCE Journal of Structural Engineering*, Vol. 120, No. 8, pp. 2377-2398.
- Bazant, Z.P. & Planas, J., 1998, *Fracture and Size Effect in Concrete and Other quasi-brittle Materials*, CRC Press, Boca Raton and London, pp. 616.
- Kim, D. J., Naaman, A. E. & S. El-Tawil, 2008, Comparative flexural behavior of four fiber reinforced cementitious composites, *Cement and Concrete Composites*, Vol.30, No.10, pp.917-928.
- Kim, D. J., Naaman, A. E. & S. El-Tawil, 2008, High tensile strength strain hardening FRC composites with less than 2% fiber content, *Proceedings of Second International Symposium on Ultra High Performance Concrete*, Germany, E. Fehling, M. Schmidt and S. Stürwald, Co-Editor, Kassel University Press GmbH, Heft 10, No. 10, pp. 169-176
- Lepech, M. & Li, V. C., 2004, Size Effect in ECC Structural Members in Flexure, *Proceedings of FRAMCOS-5*, Vail, Colorado, USA, pp. 1059-1066.
- Naaman, A. E. & Reinhardt, H. W., 1996, Characterization of High Performance Fiber Reinforced Cement Composites,

- Proceedings of 2nd International Workshop on HPFRCC*, A. E. Naaman and H. W. Reinhardt, eds., RILEM, No. 31, pp. 1-24.
- Naaman, A. E., 2003, Strain Hardening and Deflection Hardening Fiber Reinforced Cement Composites, *High Performance Fiber Reinforced Cement Composites (HPFRCC-4)*, A.E. Naaman and H.W. Reinhardt, Editors, RILEM Publications, Pro. 30, pp. 95-113.
- Soronakom, C. & Mobasher, B., 2007, Closed-Form Moment-Curvature Expressions for Homogenized Fiber-Reinforced Concrete, *ACI Materials Journal*, Vol. 104, No. 4, pp. 351-359.
- Soronakom, C. & Mobasher, B., 2008, Correlation of tensile and flexural responses of strain softening and strain hardening cement composites, *Cement and Concrete Composites*, Vol. 30, pp. 465-477.
- Ward, R. & Li, V.C., 1990, Dependence of Flexural Behavior of Fiber Reinforced Mortar on Material Fracture Resistance and Beam Size, *ACI Materials Journal*, V. 87, No. 6, pp. 627-637.